

# Neuro Fuzzy Controller for Grid Connected Photovoltaic System with Multilevel Inverter

P. Karuppusamy, A. M. Natarajan

**Abstract** – In recent years power quality is the major issue considered in the power operating devices. Because nowadays power operating applications can be increased, which causes power quality disturbances. The power quality degradation caused voltage deviation and unbalanced voltage in the system. To reduce the power quality disturbance and improve that are the difficult tasks. It is overcome by using a large number of Power electronics devices. Here we proposed the voltage regulation of the grid connected photovoltaic system using a neuro fuzzy controller. It could regulate the voltage at the grid side. This proposed technique consists of photovoltaic cell, that could produce dc voltage and the multilevel inverter has been used for the dc-ac conversion. This proposed technique neuro fuzzy controller used for the pulse generation, in which we have three layers input layer, hidden layer, output layer. The grid output voltage and the difference voltage (difference between photovoltaic voltage and the grid voltage) is the two inputs of the neuro fuzzy controller input layer. Depends on the fuzzy rules, the controller has been trained. The output layer of the neuro fuzzy controller is the controlled voltage, which generate the appropriate gate pulses. This is used to operate the multilevel inverter, it makes the proper conduction in the multilevel inverter. Finally it results regulated voltage has been maintained at the grid side.  
**Copyright © 2013 Praise Worthy Prize S.r.l. - All rights reserved.**

**Keywords:** Neuro Fuzzy Controller, Multi Level Inverter, Photo Voltaic Cell (PV Cell), Power Quality, Voltage Regulation

## Nomenclature

$V_g$	Actual grid voltage
$V_p$	Photovoltaic output voltage
$V_d$	Difference voltage
$V_{cv}^N$	Control voltage
$q$	Charge of the electron
$k$	Boltzmann's constant
$T$	Cell temperature
$D$	Solar cell diode
$R_s$	Diode present in the solar cell
$N_s$	Number of cells in the PV
$I_{mp}$	Current value at maximum power
$m$	Cell recombination coefficient
$I_s$	Current produces from the solar cell
$I_d$	Diode current of the solar cell
$V_{dc}$	Source voltage of each bridge

## I. Introduction

In renewable energy sources, the continuous economic development of many countries and the environmental issues observed in the last decades forced an intense research.

Due to their considerable advantages [1], such as reliability, reasonable installation and energy production costs, low environmental impact, capability to support micro grid systems and to connect to the electric grid [3] Hydro, photovoltaic (PV) and wind energy conversion are the most explored technologies. The PV is pointed out as one of the most modular and environmentally friendly technologies, among these energy sources [2].

For enabling electricity access for those people, and also for remote applications, the stand-alone PV system is an interesting alternative [4] and [5].

In photovoltaic systems, by PV arrays solar energy is changed into electrical energy [6]. Since PV arrays are clean, inexhaustible and involve little maintenance, they are very popular. Between the PV arrays and the grid, Photovoltaic systems require interfacing power converters [7]. For two major tasks these power converters are used they are to ensure that the PV arrays are operated at the maximum power point (MPPT) [8] and [9] and to inject a sinusoidal current into the grid. In general there are two power converters [10], [11]. The first one is a DC/DC power converter that is used to operate the PV arrays at the maximum power point.

The other one is a DC/AC power converter to interconnect the photovoltaic system to the grid [12].

Over a conventional two level converter such as: reducing switching frequency, output voltage with very low distortion and reduced dv/dt stress, multilevel power

converters present several advantages [13]. Several multilevel topologies have been applied to photovoltaic systems in this way [15], [27].

Neutral-point-clamped and flying-capacitor MLIs, requiring only one dc source, and cascaded H-bridge MLI (CHB-MLI) are the three basic MLI topologies requiring separate dc sources. The latter characteristic, which is a disadvantage when a single dc source is available, becomes a very attractive feature in the case of PV systems, because solar cells can be assembled in a number of separate generators [16], [26]. In this way, they convince the necessities of the CHB-MLI, obtaining additional advantages such as a possible removal of the dc/dc booster, a major reduction of the power drops caused by sun darkening, and, as a result, a potential increase of efficiency and reliability [19]. A noteworthy problem in multilevel converter design is the complexity of their control and of their pulse width modulator. [17] and [18]. The multilevel inverter control conventional space-vector PWM current regulator implementation is generally computationally complex. [20].

## II. Recent Research Works: A Brief Review

In literature many related works are already available which is based on multilevel inverter with photovoltaic applications. Some of them reviewed here. Carlo Cecati *et al.* [21] have investigated a converter for photovoltaic (PV) systems frequently consist of two stages: a dc/dc booster and a pulse width modulated (PWM) inverter.

They proposed a single-phase H-bridge multilevel converter for PV systems governed by a integrated fuzzy logic controller (FLC)/modulator. The novelties of the proposed system were the use of a fully FLC and the use of an H-bridge power-sharing algorithm. The majority of the required signal processing was performed by a mixed-mode field-programmable gate array, resulting in a fully integrated System-on-Chip controller. The general architecture of the system and its chief performance in a great spectrum of practical situations were offered and discussed.

R. Seyezhai *et al.* [22] have presented a Multilevel Inverter (MLI). This is developed as an attractive topology for high voltage DC-AC conversion. For a hybrid multilevel inverter employing Silicon carbide (SiC) switches for fuel cell applications, they focus on a dual reference modulation technique. As the carrier waveform the proposed modulation technique employs two reference waveforms and a single inverted sine wave. In terms of output voltage spectral quality and switching losses, this technique was compared with the conventional dual carrier waveform. The performance of the inverter has been analyzed and compared with the result obtained from theory and simulation.

R.Chandralekha *et al.* [23] have discussed the optimization in a joint power system with solar cell subsystem, wind turbine driven induction generator sub system and diesel Generator set.

Continuous power supply can be ensured by these sub-systems used in tandem and with battery backup. Solar cells would have the limitation of power generation during day time only while the wind turbine driven IG to a local community will have fluctuations in power generation due to difference in wind velocity. To consumers living in remote localities like villages in hill tops where grid supply may not exist, the combination provided continuous power supply. For obtaining a constant voltage and constant frequency a.c. power supply for utility and commercial applications the power electronic scheme proposed which involves a choice of power source inverter.

C. Vijayalakshmi *et al.* [24] have discussed about the project based on a high conversion ratio hybrid DC-DC converter fed single-phase low harmonic distortion nine-level photovoltaic (PV) inverter topology for PV power conditioning systems with a pulse width-modulated (PWM) control scheme.

To keep the current injected into the grid sinusoidal and to have good dynamic performance with rapidly changing atmospheric conditions a digital PI control algorithm is implemented in microcontroller PIC16C7F88. For low-voltage dc energy sources, a power conditioning system (PCS) is required before making it to ac for grid tie applications to change the energy sources to a higher-voltage dc. The aim of this project is to introduce and discuss the main features of these relatively new circuit topologies that deal with these practical design issues.

M. Raghu Vamsi Goutham *et al.* [25] have proposed a three-phase cascaded H-bridge converter. This converter is designed for a stand-alone photovoltaic (PV) application. The multilevel topology consists of several H-bridge cells connected in series, each one connected to a string of PV modules. The adopted control scheme permits the independent control of each dc-link voltage, enabling, in this way, the tracking of the maximum power point for each string of PV panels. Moreover, low ripple sinusoidal-current waveforms are generated with almost unity power factor. The topology offers other advantages such as the operation at lower switching frequency or lower current ripple compared to standard two-level topologies. For different operating conditions simulation and experimental results were presented.

R. Seyezhai [26] has proposed a single-phase five-level inverter. This inverter is designed with reduced number of switches. The inverter consists of a full bridge inverter and an auxiliary circuit with four diodes and a switch. Zero, +0.5Vdc, +Vdc, -0.5Vdc and -Vdc are the five levels in which the inverter produces output voltage. For the CMLI, a novel dual reference modulation technique has been proposed. The dual carrier modulation technique uses two identical inverted sine carrier signals each with amplitude accurately half of the amplitude of the sinusoidal reference signal to produce PWM signals for the switches. Using Perturb and Observe (P&O) algorithm, Maximum Power Point (MPPT) has been tracked for PV inverter.

To progress the dynamic response of the inverter, a Proportional Integral (PI) control algorithm was implemented.

J. R. Maglin *et al.* [27] have discussed about the problems related with solar converters in the solar power system due to the participation in more number of power electronics components. They discussed the study of the behaviors of the solar PV systems and the power quality issues in converters. By the switching system of the power electronic circuit and could cause damage to power equipment on the utility side and sensitive loads on the customer side, harmonics were created.

The multilevel inverter is widely used as the most modular and environmentally friendly technologies which is reviewed from the recent research works. The multilevel inverter topology plays an important role for rectifying the switching losses, the voltage stress, the total harmonic distortion (THD) and the high switching frequency in solar power generation system. Different multilevel inverter topologies are used in solar power generation (PV). The topology is varied due to the output variation and THD of inverter; also, the topology design is a complex task.

By different essential topologies like single phase cascaded H-bridge multilevel inverter, diode-clamped multilevel inverter and single phase five level inverter the problems are overcome. For the unknown load and parameter variations, the above existing models depend on the precise topology of the system and the topologies cannot be adaptive. Very few works are presented to solve those problems and also the presented works are ineffective in literature. Therefore, to do this research work all these drawbacks have motivated.

### III. Function of the Proposed Methodology

Photo Voltaic cell (PV) using power generation and the voltage regulation of the grid side are described in the block diagram, which is shown in Fig. 1. The PV cell is used for the generation of dc power, it is series with multi level inverter, which provides dc voltage into the boosted output three phase ac voltages to the grid.

The voltage on the grid is not constant at all time. So the regulatory process was given in the circuit by adding the neuro fuzzy system. The grid voltage was sensed by the voltage sensor.

The actual grid voltage ( $V_g$ ) is given to the comparator. Also the photovoltaic output voltage ( $V_p$ ) provided to the comparator, which compares both the voltages and generates difference voltage ( $V_d$ ).

The grid output voltage ( $V_g$ ) and the difference voltage ( $V_d$ ) are given to the neuro fuzzy controller system, which provides the control voltage ( $V_{cv}^N$ ) in the form of appropriate gate pulses to the multilevel inverter.

In this way the voltage regulation is performed. The PV cell description is given in detail to the next section.III.1.

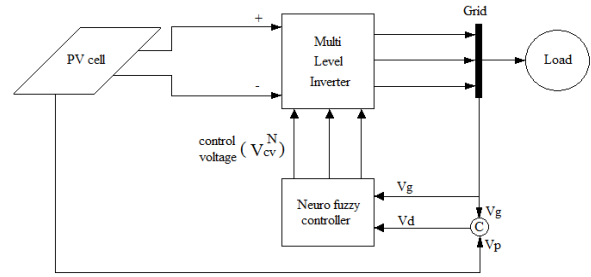


Fig. 1. Line diagram of proposed methodology

#### III.1. PV Cell Description

The PV system is used to convert the sunlight into electricity. The PV system contains solar cells. It may be grouped to form panels or arrays. The PV cells are semiconductor. The electricity produced near the top surface of the cell where the P-N junction materials are in contact. This electric field provides the force and direction to the light stimulated electrons when the sunlight strikes the surface of the PV cell. Resulting in a flow of current when the solar cell is connected to an electrical load. The current (and power) output of a PV cell depends on its efficiency and size (surface area), and is proportional to the intensity of sunlight striking the surface of the cell.

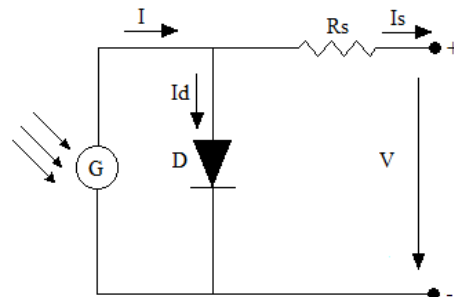


Fig. 2. PV cell equivalent circuit

The PV cell current is given by:

$$I_{pv} = \frac{I_{mp}}{1 - C^{-d}} \left[ e^{\frac{V_{oc} + q(V + R_s I)}{mkT}} - e^{\frac{V_{oc}}{a}} \right] - \frac{V + R_s I}{R_{sh}} \quad (1)$$

where,  $q$  is the electron charge ( $1.6 \times 10^{-19} C$ ),  $k$  is Boltzmann's constant ( $1.38 \times 10^{-23} J/K$ ),  $T$  is the temperature in  $K$  and  $N_s$  is the number of cells of the module,  $V_{oc} = \frac{mkT}{q} \ln \frac{I_L}{I_D}$  is the open circuit voltage,  $I_{mp}$  is the current at maximum power that is denoted by

$$I_{mp} = I_L (1 - c^{-d}) \text{ let } c = 1 + \ln \frac{I_L}{I_D} y \text{ and } d = \frac{c}{c+1}, m$$

is the cell recombination coefficient ( $1 < m < 3$ ).

Fig. 2 shows the equivalent circuit of the PV cell. Normally the solar cell is a current source. The equivalent circuit shows the solar cell with a diode  $D$  and series resistance  $R_s$ . The solar cell produces the current  $I$ . It is divided into two current values i.e., diode current  $I_d$  and output current  $I_s$ . It provides more accuracy due to the presence of series resistance  $R_s$ .

The proposed circuit was given in the following section III.2.

### III.2. Proposed H-Bridge Multilevel Inverter Working

The proposed H-bridge multilevel inverter was shown in Fig. 3. It consists of series H-bridges, which is in the order of  $h$ . The proposed system has three sections and each section produces a single phase voltage ( $V_R, V_Y$  and  $V_B$ ). It makes a three phase output voltage, in which bridge's neutral point is commonly connected to the point  $O$ . The output voltage of the proposed system is  $h$  level.

If we consider which is in the 5 level waveform circuit means the output voltage generation in each phase is given in the following Table I.

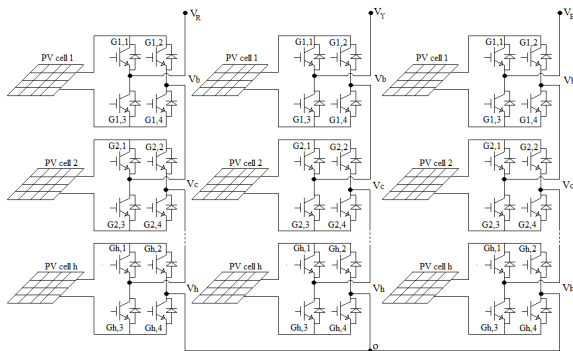


Fig. 3. Proposed H-bridge multilevel inverter

TABLE I  
LEVEL INVERTER OUTPUT VOLTAGE FOR EACH PHASE

Angle $\alpha$	$V_R$	$V_Y$	$V_B$
$0 \leq \alpha \leq \alpha_1$	0	$-V_{dc}$	$2V_{dc}/3$
$\alpha_1 \leq \alpha \leq \alpha_2$	$V_{dc}/3$	$-2V_{dc}/3$	$V_{dc}/3$
$\alpha_2 \leq \alpha \leq \alpha_3$	$2V_{dc}/3$	$-V_{dc}/3$	0
$\alpha_3 \leq \alpha \leq \pi/2$	$V_{dc}$	0	0

The above table shows the 5 level inverter output voltages of three phases, in which the  $R$  phase output voltage is ( $V_R$ ) the combination of two voltage level i.e.,  $V_b$  and  $V_c$ . In this table the switching angle  $\theta$  and the corresponding output voltages are given, the 5 level inverter output waveform is given in the Fig. 4.

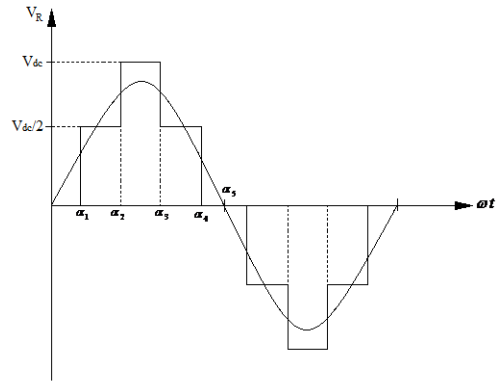


Fig. 4. Multilevel inverter fundamental frequency waveform

Similarly other two phase output voltages are illustrated in the table.

The standard multilevel inverter 5 level waveform is given in the above figure. The total output voltage is the combination of first bridge output voltage and the second bridge output voltage. The cascaded H-bridge model detailed process is given in the next section III.2.1.

### III.2.1. Model of the Cascaded H-Bridge

Normally H-bridge is an electronic circuit which enables a voltage across a load in both directions. Four semiconductor switches form an ordinary H-bridge circuit, in that the positive and negative voltage applied by a load depending on the switching action. The main advantage of the cascaded H-bridge multilevel is that it needs less number of components compare to the other two multilevel inverters like diode clamped and the flying capacitor, so the price and the weight of the inverter is less than that of the two former types. The cascaded H-bridge develops to connect more than one H-bridges in the series. Fig. 3 shows the proposed system consists of  $h$  dc generators and cascaded H-bridges.

These are arranged in a three phase multi level inverter topology. The PV cells are arranged series or in parallel with each dc generator and obtain required output voltage. Three single phase systems are connected star or delta connection can make the three phase system.

The number of the output voltage level of the H-bridge is  $2h + 1$ , where  $h$  is the number of levels. The number of levels and the H-bridges has to be chosen according to the available PV fields and design considerations. The number of levels chosen high to produce better sinusoidal voltage waveform and the current waveform. However the switching frequency reduced by increasing the number of levels compared to two level inverters.

The multi level inverter uses each H-bridge can be produced a square waveform, the inverter output voltage increases with each level. Each level of the H-bridge having different voltages. The dc capacitor was used to increase the voltage level according to the switching action. The voltage of the multilevel inverter in single phase is given by:

$$\begin{bmatrix} V_{B1} \\ V_{B2} \\ \vdots \\ V_{Bh} \end{bmatrix} = \frac{2V_{dc}}{\pi} \begin{bmatrix} V_b^1 \\ V_c^2 \\ \vdots \\ V_h^h \end{bmatrix} \begin{bmatrix} \cos \alpha_1^1 + \cos \alpha_2^1 + \cos \alpha_3^1 + \cos \alpha_4^1 \\ \cos 3\alpha_1^2 + \cos 3\alpha_2^2 + \cos 3\alpha_3^2 + \cos 3\alpha_4^2 \\ \vdots \\ \cosh \alpha_1^h + \cosh \alpha_2^h + \cosh \alpha_3^h + \cosh \alpha_4^h \end{bmatrix} \begin{bmatrix} \frac{\sin \alpha^1}{3} \\ \frac{\sin 3\alpha^2}{3} \\ \vdots \\ \frac{\sinh \alpha^h}{h} \end{bmatrix}$$

where,  $V_{B1}, V_{B2}, \dots, V_{Bh}$  is the bridge voltages,  $V_{dc}$  is the source voltage of each bridge,  $\alpha_1^i, \alpha_2^i, \alpha_3^i, \alpha_4^i$ ,  $i = 1, 2, 3, 4$  is the switching angles,  $1, 3, \dots, h$  harmonic order.

The inverter output voltage in single phase is given by:

$$V_R = \frac{2V_{dc}}{m\pi} \sum_{j=1}^4 \left[ \sum_{m=1,3,5,\dots,h} \left[ \cos m\alpha_j^i \right] \sin m\alpha^i \right] \quad (2)$$

where,  $V_R$  is the total output voltage of the single phase,  $m$  is the harmonic order. Similarly the other two phase voltages are determined, so the total grid voltage can be represented by:

$$V_g = V_R \sin(\alpha) + V_Y \sin(\alpha - 2\pi/3) + V_B \sin(\alpha - 4\pi/3) \quad (3)$$

The above equation is the multilevel inverter output voltage, which is given to the grid i.e., grid voltage  $V_g$ .

The grid voltage is regulated by using the neuro fuzzy controller.

The Neuro fuzzy controller input is grid voltage  $V_g$  and the difference voltage  $V_d$  (difference between PV voltage  $V_p$  and the grid voltage  $V_g$ ).

The difference voltage generated according to the time instants, the random generation of different voltage and the corresponding grid voltage is provided to the neuro fuzzy controller. The random generation of difference voltage generation is illustrated by the following equation:

$$\begin{bmatrix} V_d^{t1} \\ V_d^{t2} \\ \vdots \\ V_d^{th} \end{bmatrix} = \begin{bmatrix} V_g^{t1} - V_{pv}^{t1} \\ V_g^{t2} - V_{pv}^{t2} \\ \vdots \\ V_g^{th} - V_{pv}^{th} \end{bmatrix} \quad (4)$$

where,  $t_1, t_2, \dots, t_h$  is the pulse timing for the voltage generation.

The random generation of the grid voltage is given by the following Eq. (5):

$$\begin{bmatrix} V_g^{t1} \\ V_g^{t2} \\ \vdots \\ V_g^{th} \end{bmatrix} = \begin{bmatrix} V_R \sin(\alpha)^{t1} + V_R \sin(\alpha - 2\pi/3)^{t1} + V_R \sin(\alpha - 4\pi/3)^{t1} \\ V_R \sin(\alpha)^{t2} + V_R \sin(\alpha - 2\pi/3)^{t2} + V_R \sin(\alpha - 4\pi/3)^{t2} \\ \vdots \\ V_R \sin(\alpha)^{th} + V_R \sin(\alpha - 2\pi/3)^{th} + V_R \sin(\alpha - 4\pi/3)^{th} \end{bmatrix}$$

The above input Eqs. (4) and (5) are used to train the neural network. In this training data generate the fuzzy rules. Depending upon the fuzzy rules the controlled output voltage  $V_{cv}^N$  was produced, which is given to the multilevel inverter in the form of gating pulses.

According to the controlled gating pulses the output voltage is developed, which regulates voltage. The detailed explanation of the neuro fuzzy controller given in the next section III.3.

### III.3. Neuro Fuzzy Controller

Neuro fuzzy is in the field of artificial intelligence, which is the combination of artificial neural networks and fuzzy logic. The neural network is used to develop the training dataset and testing for the input data applied.

The proposed method feed forward type neural network was used. Usually the neural network consists of three layers, which are (i) Input layer, (ii) Hidden layer, (iii) Output layer. The NFC have two input layers grid output voltage and the difference voltage, number of hidden layers and one output i.e., the controlled output voltage.

The controlled output voltage is used to give the appropriate gate pulses, which is used to trigger the MLI switches. This operation is used for the grid voltage control.

The NFC operation briefly described in the next section III.3.1.

#### III.3.1. Control Voltage Generation Using NFC

The two inputs are given to the input layer i.e., grid output voltage ( $V_g$ ) and the difference voltage ( $V_d$ ).

The controlled voltage ( $\Delta V_{cv}^N$ ) is the output of the neural network. The neural network process performed in the hidden layer. The neural network structure is given in Fig. 5.

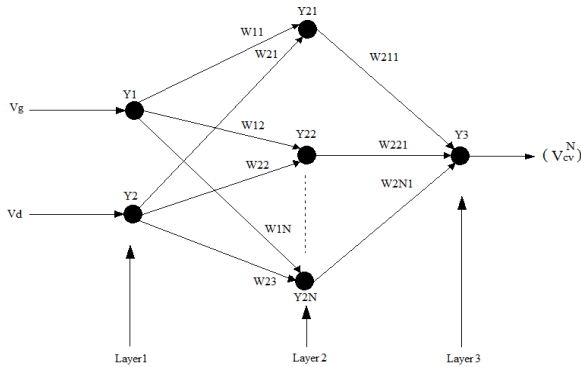


Fig. 5. Neural network structure of the proposed method

From Fig. 5, the hidden layer is represented as  $Y_{21}, Y_{22}, \dots, Y_{2N}$  and the neuron weight is denoted as  $W$ .

The input layer to hidden neuron weight is  $W_1$  and the hidden layer to output layer weight is  $W_2$ . The proposed neural network training and weight adjustment are done using the Back Propagation (BP) process. It is briefly described in the following steps.

*Step1:* Initialize all the dataset like input, output and weight of the neuron. Here the inputs of the network are grid output voltage  $V_g$  and the difference voltage  $V_d$ .

The calculated control voltage  $V_{cv}^N$  is the output of the network.

*Step2:* To determine the BP error of the input dataset  $V_g$  and  $V_d$ :

$$E_1 = V_{cv}^N T - V_{cv}^N out \tag{6}$$

where,  $V_{cv}^N T$  is the target control output voltage,  $V_{cv}^N out$  is the actual control output voltage.

*Step3:* Calculate the network output using the following relation:

$$V_{cv}^N out = \sum_{n=1}^N W_{2n1} V_{cv}^N (n) \tag{7}$$

where:

$$V_{cv}^N (n) = \left[ 1 + e^{(-W_{1n} e(n) - W_{2n} \Delta e)} \right]^{-1}$$

The both above equations are represented the output layer and hidden layer activation function respectively.

*Step4:* Find the new weights of all the neurons:

$$W_{new} = W_{old} + \Delta W \tag{8}$$

where,  $\Delta W$  is the change in weight, The change in weight can be determined by the following relation,  $\Delta W = \gamma V_{cv}^N E_1$   $\gamma$  is the learning rate which is ranging from 0.2 to 0.5.

*Step5:* The process will be repeated from 2, until the  $E_1$  gets minimized to a least value:

$$10E_1 < 1 \tag{9}$$

Once the process is completed the network is well trained and give control voltage  $V_{cv}^N$ . In this training process completed, the fuzzy rules are generated. The fuzzy rules consists of three stages like, fuzzification, decision making and defuzzification. These processes are used to produce the controlled voltage  $V_{cv}^N$ . The fuzzy rules generation is described in next section III.4.

### III.4. Development of Training Dataset Using Fuzzy Rules

The operation of the controller is mainly depends on the fuzzy rules. The fuzzy rules generated using fuzzy set theory. Fuzzy controller has three steps fuzzification, decision making, and defuzzification. During the fuzzification process crisp values are converted into fuzzy value. The triangular fuzzy set is used for this work. The output is introduced to the decision making block, which consists of a set of rules. Using the fuzzy rules makes the decision for the appropriate control voltage generated, it will be given to the defuzzification process. Defuzzification is the inverse process of the fuzzification.

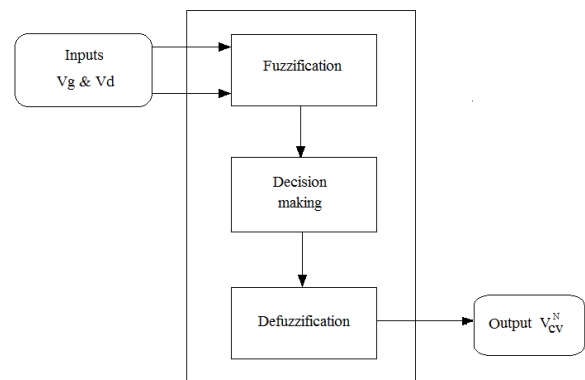


Fig. 6. Fuzzy logic controller

The designing process of the Fuzzy logic controller is given by:

1. Find out the grid voltage and the difference voltage.
2. Fuzzification process.
3. Making the decisions depending on the fuzzy rules.
4. Defuzzification process.
5. Check the output of the power operating device.

The linguistic variables of inputs grid voltage control

voltage  $V_g$ , difference voltage  $V_d$  and control voltage  $V_{cv}^N$  are Negative Big (NB), Negative Small (NS), Zero Error (ZE), Positive Big (PB) and Positive Small (PS).

These are in the rule base, which rules are tabulated in the following Table II.

TABLE II  
FUZZY RULES

$V_d \backslash V_g$	NB	NS	ZE	PS	PB
NB	ZE	NS	NB	PB	PB
NS	ZE	NS	NB	PB	PB
ZE	NS	NB	ZE	PS	PB
PS	NB	PB	NS	PS	PS
PB	NB	PB	NS	PS	PS

The above table shows the fuzzy rules, it can develop the control voltage  $V_{cv}^N$ . This control voltage develops the appropriate gate pulses, it is used to control the MLI semiconductor switches. In the proposed system discussed with the NFC, which can be performed on the MATLAB platform. The results proposed system and the explanations are given in the next section IV.

#### IV. Experimental Results and Discussions

The proposed technique was implemented in MATLAB platform. In this proposed technique, the normal grid voltage is not constant at all time. The grid voltage was sensed by the voltage sensor. The sensed actual grid voltage ( $V_g$ ) and the photo voltaic output voltage ( $V_p$ ) is given to the comparator. The comparator discovers the difference voltage ( $V_d$ ) between both the grid voltage ( $V_g$ ) and photo voltaic output voltage ( $V_p$ ). The grid output voltage ( $V_g$ ) and the difference voltage ( $V_d$ ) are given to the proposed NFC technique.

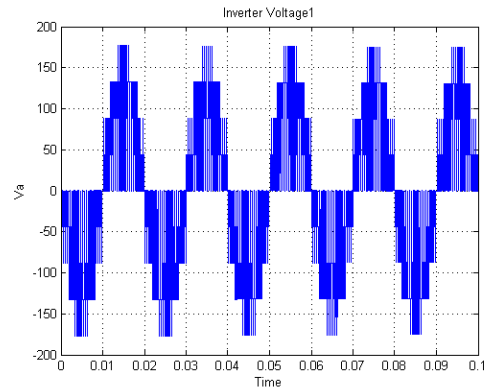
The training of the NFC and the weight adjustment of the neuron is done using the back propagation technique.

The control voltage ( $V_{cv}^N$ ) in the form of appropriate gate pulse generation mainly depends on the fuzzy rules.

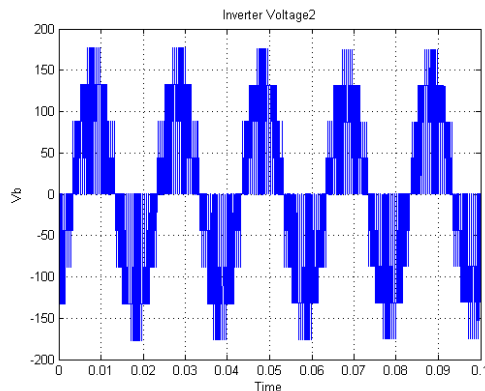
The proposed technique uses five level inverter and the corresponding results are given in the following figures. The Figs. 7(a), 7(b) and 7(c) are the standard five level inverter staircase waveforms of the phases a, b and c respectively. The normal grid voltage and the current waveforms are given in the Figs. 8(a) and 8(b) respectively. These are the normal conditions, then we noted the arbitrary generation of faults during the difference time faults. From Figs. 9(a) to 9(h) illustrates both the voltage and current distortion duration between 0.015-0.02, for without control technique, Fuzzy Logic control (FLC), Neural Network (NN) and Neuro Fuzzy control techniques respectively.

The Figs. 10(a) and 10(b) are the grid voltage and current using the proposed NFC technique, its distortion duration is between 0.02-0.025. The NFC control using the grid voltage and current with the distortion duration is between 0.03-0.035 is given in the Figs. 11(a) and 11(b).

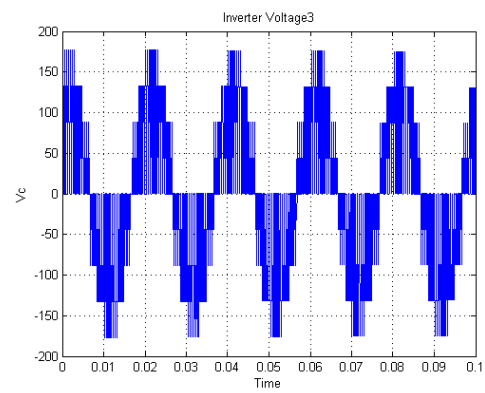
Figs. 12(a) and 12(b) show the difference distortion duration is between 0.045-0.05, using the proposed NFC controller for both the grid voltage and current. The Figs. 13(a) and 13(b) is the grid voltage and current using the proposed NFC technique, its distortion duration is between 0.047-0.05.



(a)

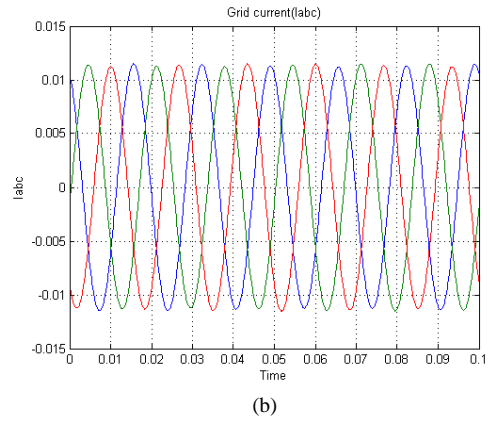
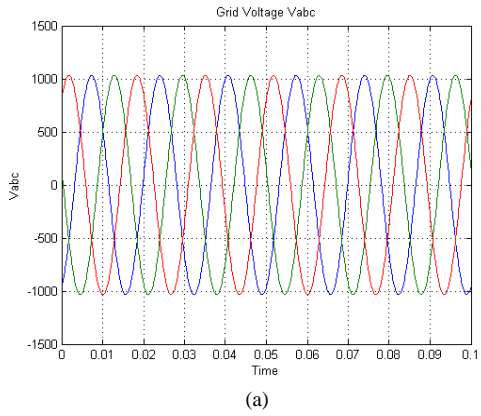


(b)

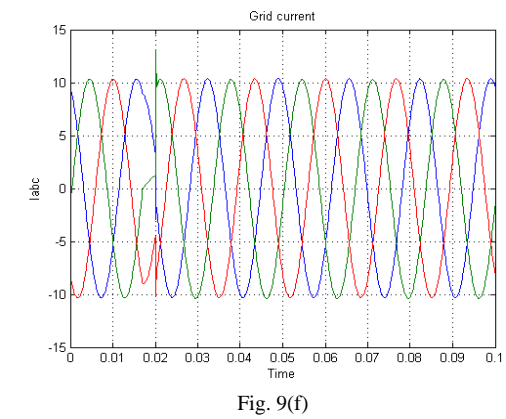
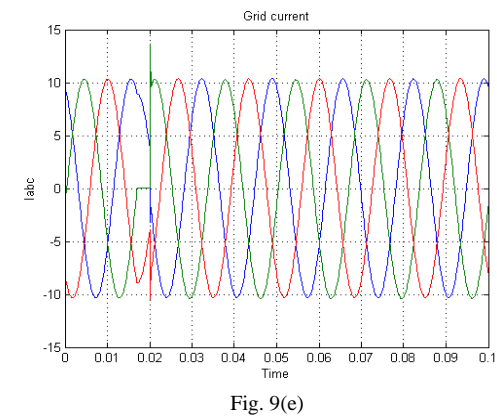
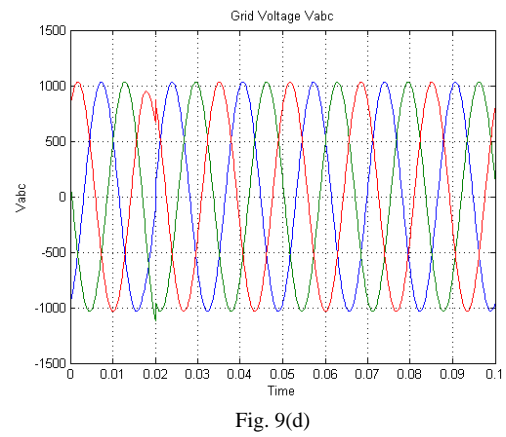
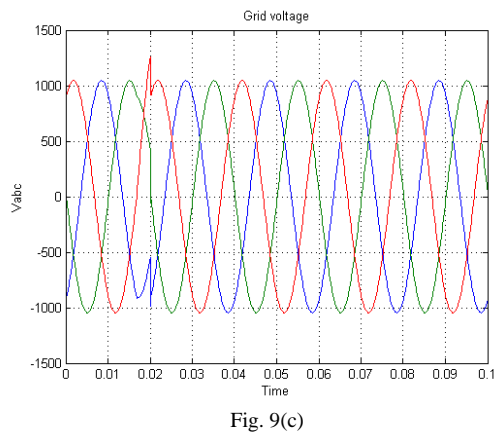
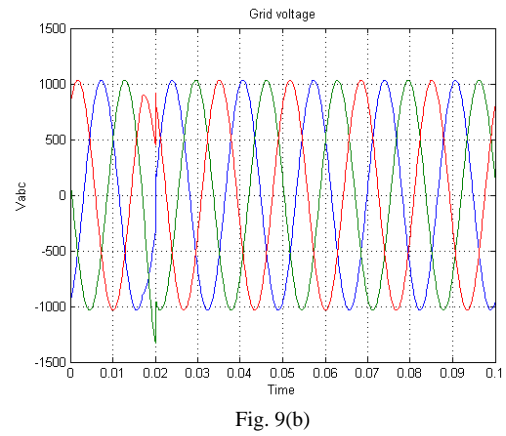
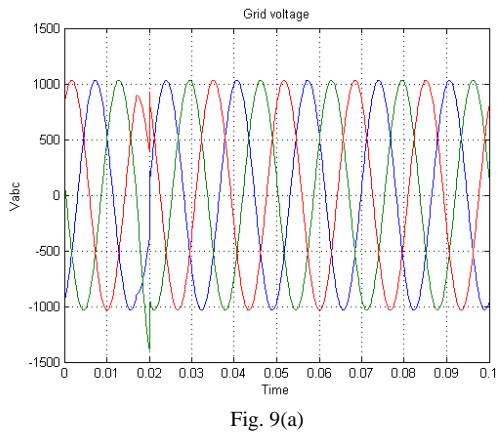


(c)

Figs. 7. (a) MLI output voltage in phase a using NFC, (b) MLI output voltage in phase b using NFC and (c) MLI output voltage in phase c using NFC



Figs. 8. (a) Grid output voltage in normal condition, and (b) Grid output current in normal condition



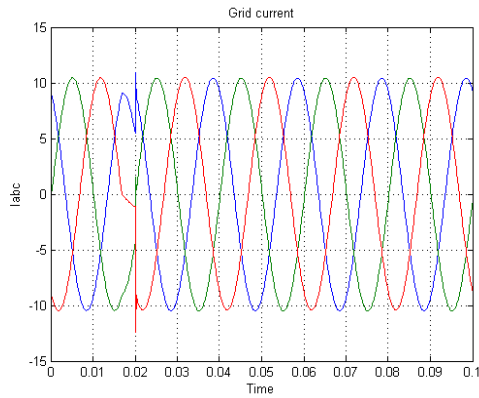


Fig. 9(g)

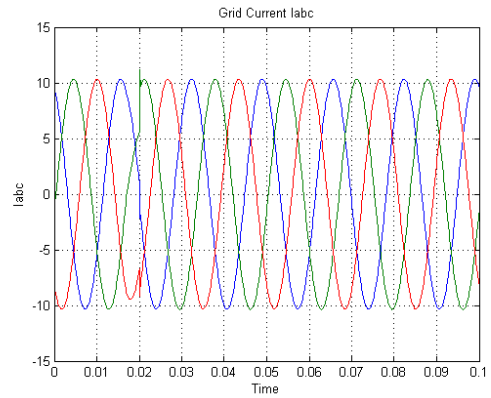
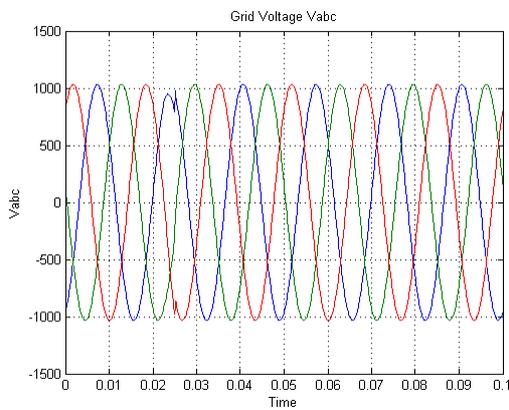
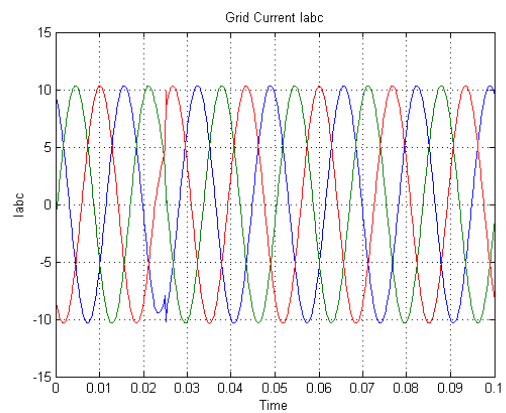


Fig. 9(h)

Figs. 9. Grid voltage and current during the Distortion time (0.015 to 0.02), (a) Grid output voltage without using control, (b) Grid output voltage with FLC, (c) Grid output voltage with NN, (d) Grid output voltage with NFC, (e) Grid output current without using control, (f) Grid output current with FLC, (g) Grid output current with NN and (h) Grid output current with NFC

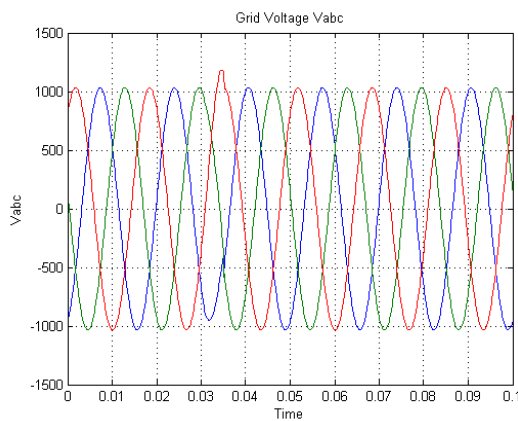


(a)

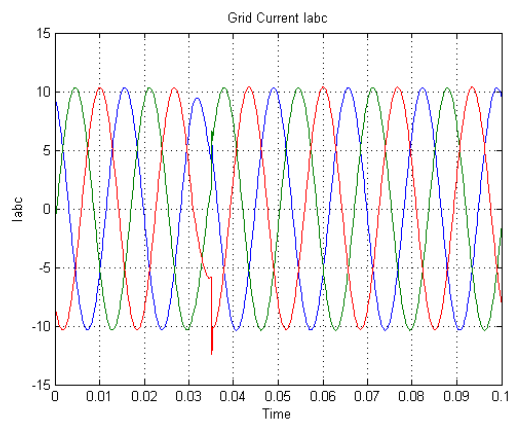


(b)

Figs. 10. Grid voltage and current during the Distortion time (0.02 to 0.025)  
(a) Grid output voltage with NFC and (b) Grid output current with NFC



(a)



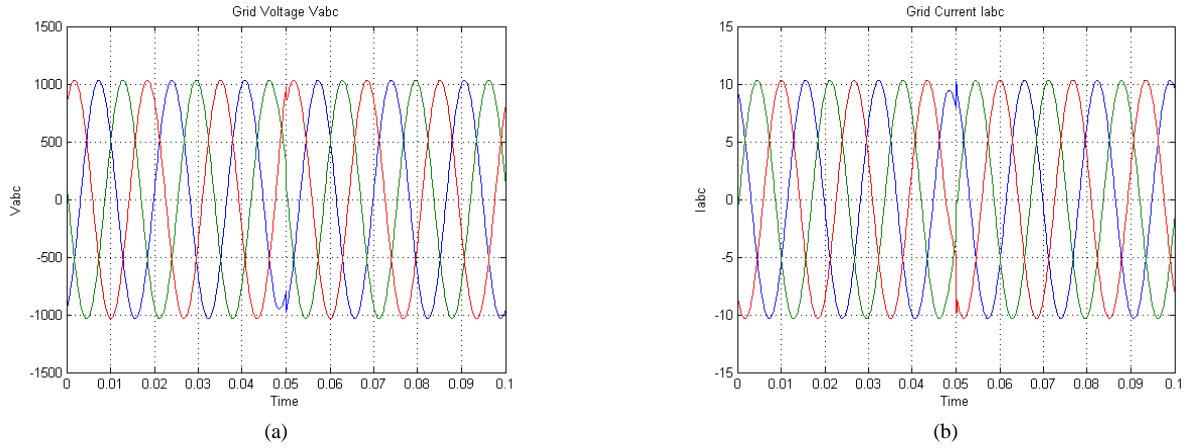
(b)

Figs. 11. Grid voltage and current during the Distortion time (0.03 to 0.035)  
(a) Grid output voltage with NFC and (b) Grid output current with NFC

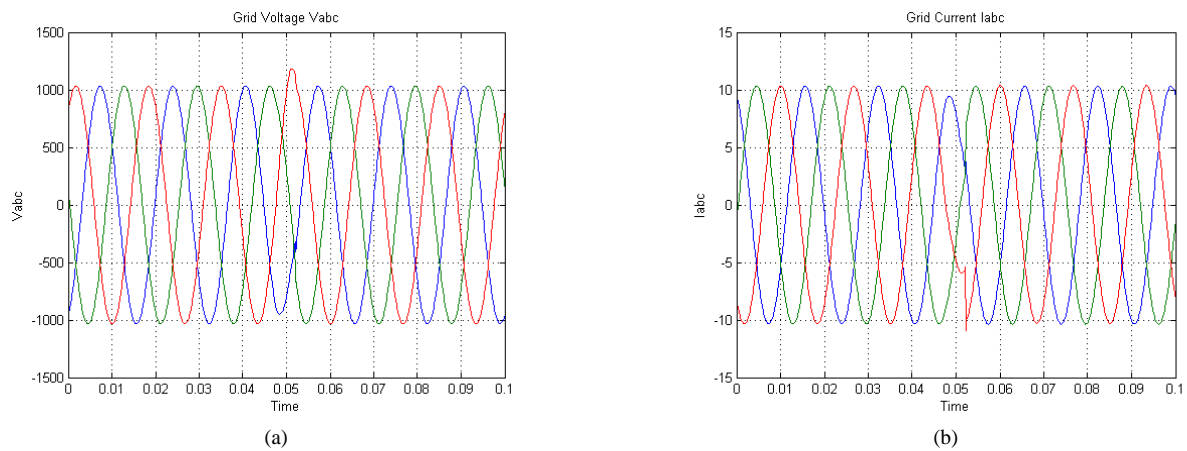
Figs. 14(a) and 14(b) shows the difference time distortion duration is between 0.049-0.054, using the proposed NFC controller for both the grid voltage and current. The NFC control using the grid voltage and

current with the distortion duration is between 0.052-0.057 is given in the Figs. 15(a) and 15(b).

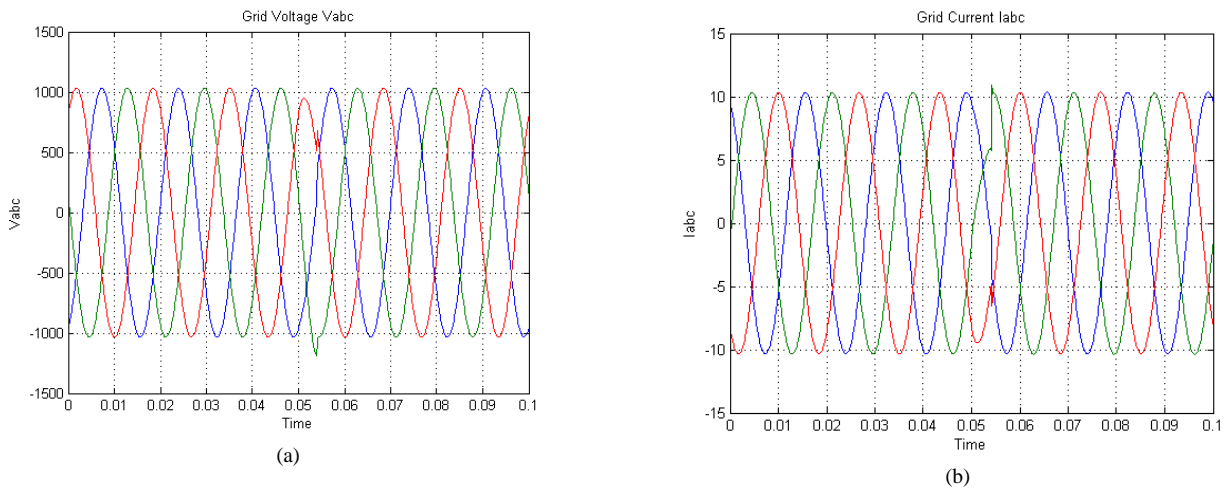
Similarly for the other techniques distortion duration is determined and the corresponding values are tabulated.



Figs. 12. Grid voltage and current during the Distortion time (0.045 to 0.05) (a) Grid output voltage with NFC and (b) Grid output current with NFC



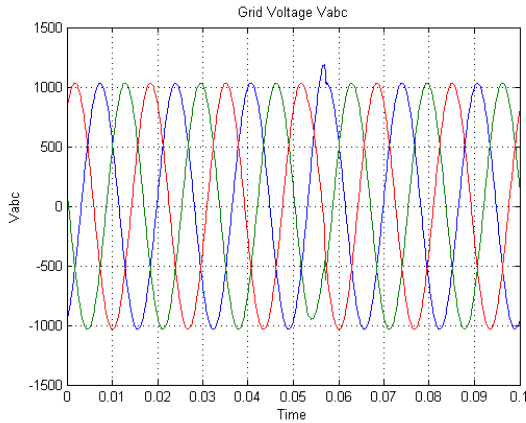
Figs. 13. Grid voltage and current during the Distortion time (0.047 to 0.052) (a) Grid output voltage with NFC, (b) Grid output current with NFC



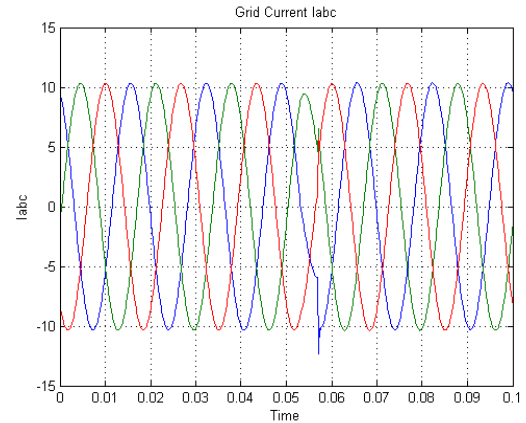
Figs. 14. Grid voltage and current during the Distortion time(0.049 to 0.054) (a) Grid output voltage with NFC and (b) Grid output current with NFC

The appropriate results for all the techniques are compared in the following Table III, which differentiate all the control techniques subjected to the different time distortions, where, DD is the distortion duration. The above table shows the difference time durations in the grid connected photovoltaic system with MLI by using various control techniques. The duration of distortion for

each technique was tabulated. In that the proposed technique is the most sufficient method of the grid connected photovoltaic system with MLI. The performance deviation of FLC and NFC, similarly the performance deviation of NN and NFC has been determined. The corresponding values are given in the following Table IV.



(a)



(b)

Figs. 15. Grid voltage and current during the Distortion time (0.052 to 0.057)  
(a) Grid output voltage with NFC and (b) Grid output current with NFC

TABLE III  
DIFFERENCE TIME FAULTS

DD	Without using control		Fuzzy Logic Control		Neural Network Control		Neuro Fuzzy Control	
	DD in Voltage	DD in current	DD in Voltage	DD in current	DD in Voltage	DD in current	DD in Voltage	DD in current
0.015-0.02	0.005	0.005	0.004	0.004	0.003	0.003	0.002	0.002
0.02-0.025	0.005	0.005	0.003	0.003	0.004	0.004	0.002	0.002
0.03-0.035	0.005	0.005	0.004	0.004	0.004	0.004	0.003	0.003
0.045-0.05	0.005	0.005	0.004	0.004	0.004	0.004	0.001	0.001
0.047-0.052	0.005	0.005	0.004	0.004	0.004	0.004	0.002	0.002
0.049-0.054	0.005	0.005	0.004	0.004	0.003	0.003	0.002	0.002
0.052-0.057	0.005	0.005	0.004	0.004	0.004	0.004	0.003	0.003

TABLE IV  
PERFORMANCE OF DEVIATION

DD	Performance deviation of FLC and NFC		Performance deviation of NN and NFC	
	Voltage in (%)	Current in (%)	Voltage in (%)	Current in (%)
0.015-0.02	50	50	33.3	33.3
0.02-0.025	33.3	33.3	50	50
0.03-0.035	25	25	25	25
0.045-0.05	75	75	75	75
0.047-0.052	50	50	50	50
0.049-0.054	25	25	33.3	33.3
0.052-0.057	25	25	25	25

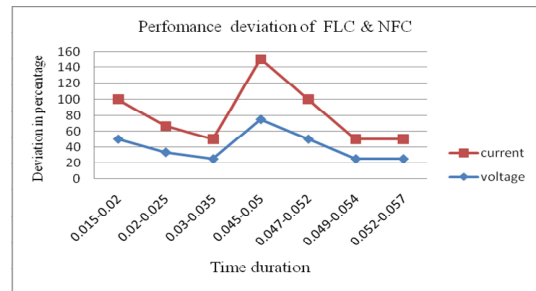
Table IV shows the both performance deviation, the voltage and current values for the techniques are given in percentage. The every values determined by the following equations. Initially the performance deviation of the FLC and NFC equation is described as the following:

$$\% \text{ of } PD_{F\&NF} = \frac{NFC - FLC}{FLC} \times 100 \quad (10)$$

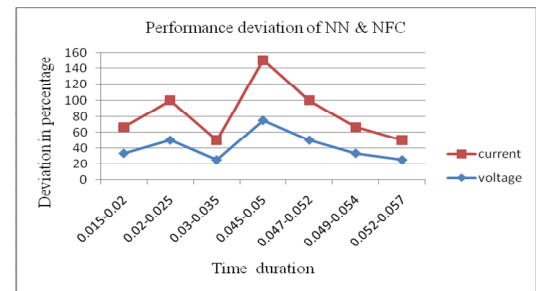
where, % of  $PD_{F\&NF}$  is the percentage of performance deviation of the FLC and NFC, similarly the performance deviation of the NN and NFC Eq. (11) is given by:

$$\% \text{ of } PD_{N\&NF} = \frac{NFC - NN}{NN} \times 100 \quad (11)$$

where, % of  $PD_{N\&NF}$  is the percentage of performance deviation of the NN and NFC. The both performance deviation is determined using the (10) and (11) equations and plotted in the graph, that is given in the Figs. 16(a) and 16(b).



(a)



(b)

Figs. 16. (a) Performance deviation of FLC and NFC and (b) Performance deviation of NN and NFC

The Figs. 16 illustrate the performance deviation of the FLC and NFC, which consists of the time duration in the x-axis and the deviation percentage in the y-axis.

The percentage of the deviation is determined by the Eq. (8). Fig. 16(b) shows the performance deviation of the NN and NFC, which is similar to the Fig. 16(a). The above results shows the deviation among NN or FLC and NFC is high. The distortion duration for the proposed technique is reduced, compared to other techniques.

## V. Conclusion

In this paper neuro fuzzy controller for grid connected photovoltaic system with multilevel inverter was discussed. Here the grid voltage and current deregulation were minimized by using the Neuro fuzzy controller. The grid output voltage and the difference output voltage were given to the input of the NFC.

The proposed NFC is already trained using back propagation algorithm depends on the fuzzy rules. The controlled output gate pulses were generated and it was given to the multilevel inverter. The output of the multilevel inverter was the five level staircase waveform, it was given to the grid.

The grid output voltage and current for the proposed NFC, NN and FLC with arbitrary time distortion were discussed. Depending on the difference time distortion for all the techniques, the proposed NFC technique is the most sufficient technique in the grid connected photovoltaic system with multilevel inverter. Because the distortion duration and also voltage deviation of the proposed technique are very low compared to other techniques. The comparative results proved that the proposed technique mitigated the voltage deviation to sufficient level which are competent over the other techniques.

## References

- [1] F. Kinninger, "Photovoltaic systems technology", Kassel, Germany: Universitat Kassel, *Institut fur Rationelle Energiewandlung*, 2003.
- [2] S. Seme, G. Stumberger and J. Vorsic, "Operational properties of a photovoltaic system with three single phase inverters", *International Conference on Renewable Energies and Power Quality*, 2010.
- [3] M. Liserre, T. Sauter, and J.Y. Hung, "Future energy systems: integrating renewable energy sources into the smart power grid through industrial electronics", *IEEE Industrial Electronics Magazine*, vol. 4, No. 1, pp. 18-37, Mar. 2010.
- [4] E. Koutroulis, K. Kalaitzakis, and N.C.Voulgaris, "Development of a microcontroller-based, photovoltaic maximum power point tracking control system", *IEEE Transactions Power Electronics*, Vol. 16, No 1, pp. 46-54, 2001.
- [5] I. Houssamo, F. Locment, and M. Sechilariu, "Maximum power tracking for photovoltaic power system: Development and experimental comparison of two algorithms", *Renewable Energy*, Vol.35, No 10, pp.2381-2387, 2010.
- [6] I.H.Altasa, and A.M.Sharaf, "A novel maximum power fuzzy logic controller for photovoltaic solar energy systems", *Renewable Energy*, vol. 33, No. 3, pp. 388-399, 2008.
- [7] Syafaruddin, E. Karatepe, and T. Hiyama, "Polar coordinated fuzzy controller based real-time maximum-power point control of photovoltaic system", *Renewable Energy*, vol. 34, No. 12, pp. 2597-2606, 2009.
- [8] C. Larbes, S. M. A. Cheikh, T.Obeidi, and A.Zerguerras, "Genetic algorithms optimized fuzzy logic control for the maximum power point tracking in photovoltaic system", *Renewable Energy*, Vol. 34, No. 10, pp. 2093-2100, 2009.
- [9] T.Tafticht, K.Agbossou, M.L.Doumbia, and A.Cheriti, "An improved maximum power point tracking method for photovoltaic systems", *Renewable Energy*, Vol. 33, No. 7, pp. 1508-1516, 2008.
- [10] A.Chaouachi, R.M.Kamel, and K.Nagasaka, "A novel multi-model neuro-fuzzy-based MPPT for three-phase grid-connected photovoltaic system", *Solar Energy*, Vol. 84, No.12, pp. 2219-2229, 2010.
- [11] N.Hamrouni, M.Jraidi, and A.Cherif, "New control strategy for 2-stage grid-connected photovoltaic power system", *Renewable Energy*, Vol. 33, No. 10, pp. 2212-2221, 2008.
- [12] A. Nabae, I.Takahashi, and H. Akagi, "A new neutral-point clamped PWM inverter," *IEEE Transactions Industry Applications*, vol. 17, No. 5, pp. 518-523, Sep./Oct. 1981.
- [13] T. A. Maynard, and H. Foch, "Multi-level choppers for high voltage applications", *European Power Electronics Journal*, Vol. 2, No. 1, pp. 45-50, March 1992.
- [14] V. Ferno Pires, J. F. Martins, D. Foito, and Chen Hao "A Grid Connected Photovoltaic System with a Multilevel Inverter and a Le-Blanc Transformer", *International Journal of Renewable Energy Research Vitor Ferno Pires*, Vol. 2, No.1, pp.84-91, 2012.
- [15] N. A. Rahim, J. Selvaraj, and C. Krismadinata, "Five-level inverter with dual reference modulation technique for grid-connected PV system", *Renewable Energy*, Vol. 35, No. 3, pp. 712-720, 2010.
- [16] K. A. Corzine and J. R. Baker, "Multilevel voltage-source duty-cycle modulation: Analysis and implementation", *IEEE Trans. Ind. Electron.*, Vol. 49, No. 5, pp. 1009-1016, Oct. 2002.
- [17] O. Lopez, A. Alvarez, J. Doval-Gandoy, and F. D. Freijedo, "Multiphase space vector PWM algorithm", *IEEE Trans. Ind. Electron.*, Vol. 55, No. 5, pp. 1933-1942, May 2008.
- [18] J. Chiasson, L.M.Tolbert, K. J. McKenzie, and Z. Du, "Control of a multilevel converter using resultant theory", *IEEE Trans. Control Syst. Technol.*, Vol. 11, No. 3, pp. 345-354, May 2003.
- [19] P. Mattavelli, L. Rossetto, G. Spiazzi, and P. Tenti, "General-purpose fuzzy controller for dc-dc converters", *IEEE Trans. Power Electron.*, Vol. 12, No. 1, pp. 79-86, Jan. 1997.
- [20] S. Saetieo and D. A. Torrey, "Fuzzy logic control of a space vector PWM current regulator for three-phase power converters", *IEEE Trans. Power Electron.*, Vol. 13, No. 3, pp. 419-426, May 1998.
- [21] Carlo Cecati, Fabrizio Ciancetta, and Pierluigi Siano, "A Multilevel Inverter for Photovoltaic Systems With Fuzzy Logic Control", *IEEE Transactions on Industrial Electronics*, Vol. 57, No. 12, December 2010.
- [22] R. Seyezhai, Banuparvathy Kalpana, and Jennifer Vasanthi "Design and Development of Hybrid Multilevel Inverter employing Dual Reference Modulation Technique for Fuel Cell Applications", *International Journal of Power Electronics and Drive System (IJPEDS)*, Vol. 1, No. 2, pp.104-112, December 2011.
- [23] R.Chandralekha, G.shasikala, and C.Sasikala, "Modeling and Analysis of Hybrid Power Systems with Power Converters", *International Journal of Advanced Engineering Sciences and Technologies*, Vol. 11, No. 21, pp. 258 - 262, 2011.
- [24] C.Vijayalakshmi, and R.Latha, "Implementation of New Single Phase Multilevel Inverter for PV Power Conditioning System", *International Journal of Advanced Scientific Research and Technology*, Vol. 2, No. 2, pp. 2249-9954, April 2012.
- [25] M. Raghuvamsi goutham and Venu gopala rao. M, "Control of a Three-Phase Cascaded H-Bridge Multilevel Inverter for Stand-alone PV System", *International Journal of Modern Engineering Research (IJMER)*, Vol. 2, No. 2, pp. 278-282, Mar-Apr 2012.
- [26] Oleschuk, V., Griva, G., Simulation of processes in synchronized cascaded inverters for Photovoltaic application, (2009) *International Review of Electrical Engineering (IREE)*, 4 (5), pp. 761-768.
- [27] Wanjekeche, T., Jimoh, A.A., Nicolae, D.V., A Novel 9-level

multilevel inverter based on 3-level NPC/H-bridge topology for photovoltaic applications, (2009) *International Review of Electrical Engineering (IREE)*, 4 (5), pp. 769-777.

### Authors' information



**P. Karuppusamy** obtained his Bachelor's degree in Electrical and Electronics Engineering from Anna University Chennai. Then he obtained his Master's degree in Power Electronics and drives from Government College of Technology, Anna University Chennai. Currently, he is an Assistant Professor (Senior Grade) in Electrical and Electronics

Engineering, Bannari Amman Institute of Technology, Sathyamangalam, Tamil Nadu, India. His specializations include Power Electronics, Solar Energy, Digital Electronics and Microprocessors.



**Dr. A. M. Natarajan**, Professor and Chief Executive, Bannari Amman Institute of Technology, Erode, Tamilnadu. He received his B.E. degree from the P S G College of Technology, Coimbatore, India in 1968, the M.Sc. degree from the P S G College of Technology in 1970 and Ph.D. degree from P S G College of Technology, Coimbatore, India in

1994. He has 42 years of experience in Academic- Teaching, Research and Administration. He received "Best Engineering College Principal Award In India-2000" Instituted by Bharatiya Vidya Bhavan ,Mumbai ,awarded by Indian Society for Technical Education , New Delhi. He also received "Best Outstanding Fellow Corporate Member Of Computer Engineering Division-2001" from The Institute of Engineers (India), Coimbatore. And he was awarded "Jaya Best Principal Award-2007" by Jaya Engineering College, Thiruninravur for outstanding contribution to Technical Education over 37 years. He is the member in the Academic Council of the Anna University, Chennai. He is also a member in the Board of Studies, Anna University Chennai & Coimbatore. He is a member in ISTE, IEEE, IEI, ACM, CSI, CII etc. He had published 45 papers in National and International Journals and 85 papers in the National and International Conferences. He authored and published 10 Books.